swan
Sustainable Water ActioN

CAPACITIES

Seventh Framework Program
FP7 Grant Agreement
INCO-20011-7.6

Deliverable 1.2

"Urban Effects on Regional Climate: A Case Study in the Phoenix and Tucson Sun Corridor"

cnrs

ARIZONA

UWE BRISTOL University of the West of England

UNIVERSIDAD DE SEVILLA

UNESCO-IHE Institute for Water Education

Authors: Zhao Yang (UA), Francina Dominguez (UA), Hoshin Gupta (UA), Xubin Zeng (UA) and Laura Norman (USGS)

Cover picture captions:

Top picture: Virgin River, Zion Canyon, Utah (USA)
Source: Maria A. Sans-Fuentes

Bottom picture: Hoove Dam, Arizona (USA)
Source: Maria A. Sans-Fuentes

Project Title	**Sustainable Water Action Network - SWAN**	
Grant Agreement	**294947**	
Deliverable title	**Urban Effects on Regional Climate: A Case Study in the Phoenix and Tucson 'Sun' Corridor**	
Deliverable name	DELIVERABLE 1.2	
Authors		
Reviewers		
Due date of deliverable	February, 2015	
Actual submission date	February, 2016	
Dissemination level		
X	PU	Public
	PP	Restricted to other program participants (including the Commission Services)
	RE	Restricted to a group specified by the consortium (including the Commission Services)
	CO	Confidential, only for members of the consortium (including the Commission Services)

Deliverable status version control		
Version	**Date**	**Authors**
V1	26 FEB 2016	Zhao Yang (UA), Francina Dominguez (UA), Hoshin Gupta (UA), Xubin Zeng (UA) and Laura Norman (USGS)

Table of Contents

NOTE **5**

MANUSCRIPT **6**

ABSTRACT **7**

1. INTRODUCTION **8**

2. METHODOLOGY **11**

2.1 WRF Model and Configuration **11**

2.2 Study Domain **12**

3. RESULTS **16**

3.1 Evaluation of Model Performance **16**

3.2 Urban Impacts on Temperature **16**

3.3 Urban impacts on precipitation **18**

3.3.1 Urban impacts on summer mean precipitation 18

3.3.2 Urban Impacts on Precipitation Occurrences 20

3.4 Urban impacts on water and energy demand 20

4. CONCLUSIONS **23**

5. REFERENCES **26**

Tables **29**

Figures **30**

Supplemental Materials **43**

NOTE

This deliverable (D1.2), originally entitled “Integrative hydrological modeling under climate change” is a publication that have been submitted to the journal ***Earth Interactions*** (a journal of the American Meteorological Society) and it has been accepted with the title *“Urban Effects on Regional climate: A Case Study in the Phoenix and Tucson ’Sun’ Corridor”*.

Earth Interactions (*EI*) is an online journal dealing with the interactions between the lithosphere, hydrosphere, atmosphere, and biosphere in the context of global issues or global change. *Earth Interactions* is an Open Access Journal, with an Impact factor of 1.84.

The manuscript is already available online at http://journals.ametsoc.org/doi/abs/10.1175/EI-D-15-0027.1, in ‘Early online Releases’. The version included in this deliverable is the final version submitted for publication and the Supplementary material.

MANUSCRIPT

Urban Effects on Regional Climate

A Case Study in the Phoenix and Tucson 'Sun' Corridor

Zhao Yang, [1] Francina Dominguez,[1*] Hoshin Gupta,[2] Xubin Zeng[1] and Laura Norman[3]

Zhao Yang, Department of Atmospheric Science, University of Arizona, Tucson, Arizona, USA.

Email: yangz@atmo.arizona.edu

Francina Dominguez, Department of Atmospheric Science, University of Illinois, Urbana, Illinois, USA. Email: francina@illinois.edu

Hoshin Gupta, Department of Hydrology and Water Resources, University of Arizona, Tucson, Arizona, USA. Email: hoshin.gupta@hwr.arizona.edu

Xubin Zeng, Department of Atmospheric Science, University of Arizona, Tucson, Arizona, USA. Email: xubin@atmo.arizona.edu

Laura Norman, U.S. Geological Survey, Western Geographic Science Center, Tucson, Arizona, USA. Email: lnorman@usgs.gov

[1]Department of Atmospheric Science, University of Arizona, Tucson, Arizona, USA.

[2]Department of Hydrology and Water Resources, University of Arizona, Tucson, Arizona, USA.

[3]U.S. Geological Survey, Western Geographic Science Center, Tucson, Arizona, USA.

ABSTRACT

Land use and land cover change (LULCC) due to urban expansion alter the surface albedo, heat capacity, and thermal conductivity of the surface. Consequently, the energy balance in urban regions is different from that of natural surfaces. To evaluate the changes in regional climate that could arise due to projected urbanization in the Phoenix-Tucson corridor, Arizona, we applied the coupled WRF-NOAH-UCM (which includes a detailed urban radiation scheme) to this region. Land cover changes were represented using land cover data for 2005 and projections to 2050, and historical North American Regional Reanalysis (NARR) data were used to specify the lateral boundary conditions. Results suggest that temperature changes will be well defined, reflecting the urban heat island (UHI) effect within areas experiencing LULCC. Changes in precipitation are less robust, but seem to indicate reductions in precipitation over the mountainous regions northeast of Phoenix and decreased evening precipitation over the newly-urbanized area.

Keywords: urbanization; land use, climate impact; water demand; energy demand

1. INTRODUCTION

Since 1950, the metropolitan region of Phoenix, Arizona, has been one of the fastest-growing urban areas in the United States (Chow et al. 2012). It has undergone substantial land use and land cover change (hereafter, LULCC) since World War II, by shifting economic priorities from a mostly agrarian lifestyle to an urbanized one. The most rapid development began around 1970, when the baby-boom generation reached adulthood, with a large number of job opportunities becoming available in the metropolitan area. By 2010, Phoenix (as the largest populated city in Arizona) had reached a population of 1.4 million, and an urban extension of 1,338.26 km^2 in 2010 (US Census, 2010). Meanwhile, Tucson has become the second-largest city with an area of 588 km^2 and a population of about 520,116 (US Census, 2010). With continuing development, both cities are projected to grow towards each other, developing into what has been called the "Arizona Sun Corridor". By the year 2050, the "Sun Corridor" is projected to develop (under the most intense urbanization scenario) as shown in figure 1, at the expense of agricultural and native semi-desert landscapes. Recent research has suggested that the impact of projected urbanization on summer-season local to regional temperature could be *as significant* as those induced by large scale-climate change (Georgescu et al. 2012).

Since 1970, summers in U.S. urban areas have been recorded as being progressively warmer under the synergistic effects of global warming and urban heat island effect (NCDC, http://www.ncdc.noaa.gov/cag/). The 2014 Climate Central report indicates that 57 out of 60 the largest cities U.S. cities had measurable growth in urban heat island effect over the period 2004 to 2013 (Climate Central, 2014). For Phoenix and Tucson, the mean temperatures are 1.8 °C and 0.22 °C warmer, respectively, than in their surrounding rural areas (Climate Central, 2014), and the temperature in the Phoenix urban core has been reported as being 2.2 °C higher compared to the surrounding area (Brazel et al. 2007). The most significant effect of urbanization of temperature (due to the urban heat island effect) has been found to occur at night, with minimum temperatures in Phoenix and Tucson being (on average) 3.8 °C and 1.3 °C respectively warmer than the surrounding rural area (Brazel et al. 2007). Svoma and Brazel (2010) reported that the daily minimum temperature is most strongly influenced by urbanization, with the mean minimum temperature during the urban period exceeding that of the pre-urban period by 4.4 °C.

In addition to the heat island effect, urbanization may also affect regional climate by changing local circulation and precipitation patterns. Evidence from many observational studies suggests that urbanization can bring about modifications to rainfall patterns over and downwind of cities (Burian and Shepherd 2005; Changnon et al. 1977; Shepherd 2005, 2006). In the early 1970s, the Metropolitan Meteorological Experiment (METROMEX) showed that urbanization can lead to increased precipitation during the summer season (Changnon et al. 1977; Huff and Vogel 1978), with about 5% - 25% increases in observed precipitation over and within 50-75 km downwind of the urban area (Changnon 1979; Changnon et al. 1981; Huff and Vogel 1978). Shepherd (2006) studied a 108-year precipitation historical data record for Arizona, and found statistically significant increases in mean precipitation of 11-14% in the Lower Verde basin (northeast of Phoenix) from a pre-urban (1895-1949) to post urban (1950-2003) period associated with the expansion of the Phoenix metro area. Studies also suggest that cities can also modify the diurnal distribution of precipitation. For instance, Balling and Brazel (1987) reported the more frequent occurrence of late-afternoon storms in Phoenix during recent years; however, they did not find evidence for significant changes in the mean precipitation amounts and frequencies during the entire summer monsoon season.

Several modeling studies have investigated the effects of urbanization on precipitation. Baik et al. (2001) investigated dry and moist convection forced by an urban heat island (UHI) effect using a 2-D, non-hydrostatic, compressible model, and concluded that increased urban heat island effect can decrease the time required for rainwater formation, while moving the horizontal location closer to the heating center. Craig and Bornstein (2002) found that the UHI can induce convergence and convection. Using the Weather Research and Forecast (WRF) model, Lin et al. (2011) found that the UHI can affects the location of thunderstorms and precipitation in northern Taiwan. Veerbeek et al. (2011) found that extreme rainfall over the cities of Beijing, Mumbai and Can Tho has been increasing, and suggested that significant changes in flood risk and precipitation levels will likely occur.

Over our region of interest, Georgescu et al. 2008 used the Regional Atmospheric Modeling System (RAMS) to simulate 3 different dry and 3 different wet years with land surface data circa 1973, 1992, and 2001 over the Phoenix metro region. They concluded that the signal of increasing precipitation due to LULCC is present only during dry years. Georgescu et al. (2009a, 2009b) investigated the mechanism of precipitation enhancement and concluded that

precipitation recycling, rather than the direct or indirect effect of the urbanization, may be responsible for the precipitation increase.

While numerous studies such as those mentioned above suggest an enhanced signature of precipitation over and downwind of metropolitan areas, there remain reasons to be skeptical. Precipitation anomalies in the La Porte station, Indiana, studied extensively in the METROMEX program, began to shift locale in the 1950s and then disappeared in the 1960s (Changnon et al. 1980). Tayanç et al. (1997) found no evidence of urban effects on precipitation for four large cities in Turkey. And, a study of the Pearl River Delta of China actually reported reductions in precipitation (Kaufmann et al. 2008). Despite decades of work it remains unclear why the UHI can enhance precipitation in some regions while seemingly having no effect, or leading to decreases, in other regions.

This paper investigates temperature and precipitation variations over the state of Arizona that may arise due to projected urban expansion of the Phoenix-Tucson “Sun Corridor”. To understand the causes for potential temperature and precipitation changes over the urban and downwind regions, we employ a numerical modeling framework to examine the changes that may arise due to projected future expansion. We use the non-hydrostatic, compressible Weather Research and Forecasting model (WRF), and account for urban characteristics by incorporating an Urban Canopy Model (UCM). Our study is similar to the work of Georgescu et al. 2012 and 2013 in that we use the WRF+UCM to study the effects on regional climate in the “Sun Corridor” region. However, our goal is to examine the hydroclimate of the entire corridor region in detail, with our hypothesis being that detailed representation of the hydroclimate of the region can lead to better characterization of the impacts of urbanization on precipitation. To this end, we use a high-resolution simulation that does not require a convective parameterization, and so is able to more accurately represent convective events during the monsoon season; i.e., our simulations are at a 2km resolution, while Georgescu et al. 2012 and 2013 use 20km resolution.

In the next section we introduce the numerical model and experimental design. Section 3 presents and discusses results from two land use scenarios, and reports additional analysis regarding the potential impacts of LULCC on future water and energy demand variation. A summary and our conclusions appear in section 4.

2. METHODOLOGY

This study uses the WRF model to simulate regional climate with two different land use scenarios - one with historical observed land cover for 2005, and the other for projected future land cover. We perform simulation during the peak summer monsoon season (i.e., July and August) for each year from 1991 to 2000.

2.1 WRF Model and Configuration

The WRF model version 3.4 is coupled to a land surface and urban modeling system that aimed to address emerging issues in urban areas (Skamarock et al. 2008). Our experiment uses the Noah LSM to model the land surface (Chen and Dudhia 2001), thereby providing surface energy fluxes and surface skin temperatures that serve as the boundary conditions for the atmospheric model. While the original version of Noah LSM has a bulk parameterization for urban land use, our experiment uses a single layer urban canopy model (UCM) to better represent the energy fluxes and temperature within the urban region. This single-layer urban canopy model, first developed by Kusaka et al. (2001) and further modified by Kusaka and Kumura (2004), consists of 2-dimensional symmetrical street canyons of infinite length, with treatment of momentum and energy that considers the canyon orientation and the diurnal variation of azimuth angle (Tewari et al. 2006). The UCM model estimates temperature, energy fluxes at roof, wall, and road surfaces, which later serve as lower boundary conditions for the atmospheric model. It is important to point out that the UCM does not include urban irrigation. Other parameterizations applied in this experiment were chosen based on the operational WRF simulations that are continuously produced at the University of Arizona during the monsoon season – all schemes, and in particular the microphysics scheme, have been chosen to optimally represent very heavy precipitation and winds associated with the strong to severe storms during the season (M. Leuthold personal communication).The parameterizations include the Morrison double-moment scheme for microphysics (Morrison et al. 2009), the CAM scheme which allows for aerosols and trace gases for longwave and shortwave radiation (Collins et al. 2004), the Eta surface layer scheme for the surface layer parameterization and the Noah land surface model for the land surface scheme (Chen and Dudhia 2001; Janjić 1996, 2002), the Mellor-Yamada-Janjic scheme for planetary boundary layer physics (Janjić 1990, 1996, 2002; Mellor and Yamada 1982), the Kain-Fritsch convective parameterization scheme (Kain 2004) for the outer domain, and no convective parameterization for the inner domain.

2.2 Study Domain

The study region mainly covers the state of Arizona, from latitude 30.7˚ N to 35.7˚ N, and longitude 115.2˚ W to 108.2˚ W. We use 2 nested domains with outer grid spacing of 10 km and inner grid spacing of 2km (see figure 1). The inner domain has 175 grid cells in the zonal direction and 190 grid cells in the meridional direction, and is chosen to correspond to the urban area and regions that may be affected by the urban corridor (i.e., including areas at least 75 km far from the urban border).

2.3 Land Use Representation

Land use characteristics for 2005 (hereafter, LULC_2005) were obtained directly from default MODIS land use data available in the WRF model. The projected land use characteristics for 2050 (hereafter, LULC_2050) are derived by combining three different datasets, under the most intense urbanization scenario:

1) SLEUTH data: A geospatial dataset describing a future current-trends scenario of unmanaged exponential growth of land use change into the year 2050 in the Santa Cruz Watershed (Tucson area) using the SLEUTH model (named as an acronym for its input data layer requirements: slope, land use, exclusion, urban extent, transportation and hillshade data), a fuzzy constrained cellular automata model that can predict potential future urban growth in a spatially explicit fashion. The dataset has a 30-m resolution, Universal Transverse Mercator projection (Zone 12), and was created using input from local government to establish areas to be excluded from growth. The scenario predicts the footprint of urban growth to approximately triple from 2009 to 2050, which is corroborated by local population estimates (Norman et al. 2012).
2) MAG: Raster imagery describing a future scenario for 2050, for the state of Arizona, developed by the Maricopa Association of Governments (MAG, 2005). MAG staff, working with the other Councils of Governments (COGs), used a “red-dot” algorithm and input describing land ownership to establish areas to be excluded from growth, along with census information, to develop a “what if” scenario to see how the state could develop. Red dots represent housing units, which are expected to triple by 2050, from 2000, when the population is expected to hit 16 million (MAG, 2005).

3) NALC: The 2005 North American Land Cover (NALC) data, classified using MODIS data (250-m), describing current land use/land cover (Commission for Environmental Cooperation 2013).

The higher-resolution datasets (SLEUTH and MAG) were resampled to a uniform 250-m resolution to mimic the MODIS-derived NALC data, and then re-projected into Lambert Azimuthal Equal Area. The NALC data were reclassified to the MODIS 20-category land-use classification, where urban area is class #13. Urban classes from the MAG dataset for 2050 and the SLEUTH dataset for 2050 were overlain and superimposed into the MODIS-style dataset to mimic the highest resolution, most accurate future urban growth scenarios for the entire study area. This resulted in datasets describing land use/land cover for 2005 and in 2050 based on the modified IGBP-MODIS 20-category land-use classification. The datasets were converted from geospatial information systems (GIS) format into ASCII txt files, culminating in 43070 rows and 35000 columns of information, to be used as input to the WRF model. They were then super imposed on the default WRF MODIS 20-level classification scheme.

2.4 Lateral Boundary Conditions

The same climate forcings were used to drive the WRF model for the two different sets of land use data. The lateral boundary conditions were obtained from the North American Regional Reanalysis (NARR) data (Mesinger et al. 2006). Initial soil moisture and temperature conditions were also derived from NARR data. NARR provides similar soil conditions when compared with the North American Land Data Assimilation System (NLDAS) soil moisture products (not shown). We simulated each of the years from 1991 to 2000, beginning on June 15 1200Z and running through the end of August (August 31 1200Z) to cover the peak of the monsoon season in Arizona.

2.5 Observational Temperature Data

In section 3.4 we correlate urban temperatures with electricity load within Tucson and Phoenix to then be able to estimate the effect of future temperatures on electricity load under urban expansion. Near surface air temperatures collected by the Arizona Meteorological Network (AZMET) were used; AZMET provides meteorological and weather-based information for agriculture and horticulture in southern and central Arizona. The observation station for Tucson

is located at 32°16' N and 110°56' W, very close to the city center. The station for Phoenix is the Phoenix Encanto site at 33°28' N and 112°05' W. Both sites are located within the urban region in the LULC_2005, and therefore provide a good representation of actual urban temperature. Both sites provide hourly air temperature, relative humidity, wind speed and etc (data available online at http://ag.arizona.edu/azmet/).

The electric load data for Tucson were provided by the Tucson Electric Power (TEP), and for Phoenix by the Arizona Public Service (APS) and the Salt River Project (SRP). The electricity data were provided at one-minute time-step, and were aggregated to hourly time-step to correlate with the observed temperature data.

2.6 Calculation of Statistical Significance

To test for temperature and precipitation change, we performed statistical tests on their mean values. Since temperature and precipitation are highly auto-correlated, a de-correlation factor was incorporated into the statistical test using the following equation:

$$z = \frac{\overline{\Delta} - \mu_{\Delta}}{(s/\,n)^{1/2}}$$

where $\overline{\Delta} = \frac{1}{n}\sum_{i=1}^{n}\Delta i = \overline{x_1} - \overline{x_2}$, n is the sample size, x_1 and x_2 are the sample data at each grid point under different landscape representations, and μ_{Δ} = 0 since the two sample means are assumed to be the same. To account for auto-correlation, we use the effective sample size n', formulated as:

$$n' \approx n\frac{1-\rho_1}{1+\rho_1}$$

where ρ_1 is the lag 1 auto-correlation coefficient.

Statistical significance of the temperature and precipitation results was also analyzed using the bootstrap method, a useful approach for circumstances when sample sizes are small (Zoubir and Boashash 1998). This was performed as follows: 1) for each grid in each of the two landscape representations, the temperature and precipitation time series in LULC_2005 and

LULC_2050 were resampled with replacement; 2) for each (re)sample, the corresponding mean and difference in mean were recorded; 3) steps 1) and 2) were repeated 1000 times; 4) if 97.5 % of the differences were found to be larger than 0, this was considered to represent a statistically significantly increase (similarly if 97.5% of the difference were less than 0 this was considered to represent a statistically significantly decrease, and otherwise representing no significant change).

3. RESULTS

3.1 Evaluation of Model Performance

To evaluate model performance, simulations for the period 1991-2000 were compared with PRISM data (PRISM Climate Group, available online at http://prism.oregonstate.edu). Figure 2 shows that WRF simulation can reasonably downscale the spatial pattern of temperature and precipitation from the forcing NARR data. It captures the dipole pattern of precipitation distribution as well as the gradual decrease of temperature from the southwest to the northeast of the domain. After downscaling, WRF simulation tends to underestimate the domain averages for both temperature and precipitation, with WRF simulated temperature being about 0.91 °C cooler, and precipitation being about 38 mm (36%) less than PRISM for the simulated July-August period. Similarly, the original NARR data has less domain average precipitation as well (27.5mm less) but warmer average temperature (0.90 °C). Root mean square error (RMSE) of temperature is very close in both WRF (0.98 °C) and NARR (0.92 °C), but the precipitation in NARR was better with RMSE equals to 29.59 mm, comparing to 43.7 mm in WRF. Even though the WRF simulation underestimates precipitation as compared to NARR, it is important to note that precipitation in NARR is obtained from data assimilation and might not capture fine-scale precipitation features. On the other hand, due to the higher resolution in WRF, much finer details in the temperature and precipitation fields are represented. Moreover, WRF realistically captures the interannual variability of domain average temperature and precipitation (figure 3), with correlation coefficient of 0.87 for temperature variation and 0.74 for precipitation variation. Even though the magnitudes of temperature and precipitation tend to be slightly lower than the PRISM data, the WRF simulations can be treated as credible, given that they realistically capture the spatial pattern and interannual variability.

3.2 Urban Impacts on Temperature

The effects of the urban heat island on temperature are shown in Figure 4. Daily mean, maximum and minimum temperature were obtained from hourly temperature data, and then were averaged respectively during the monsoon season to represent the seasonal mean, maximum and minimum temperature. On average, changes in the mean, maximum and minimum temperature over the urbanized area are +1.27 °C, -0.07°C and +3.09°C respectively. Difference in mean daily temperature between LULC_2050 and LULC_2005, averaged over 10

years of simulation, shows a statistically significant increase over the urbanized area. While the daily maximum temperature during the daytime is not significantly altered, the minimum temperature (occurring at night) over urbanized areas shows a significant increase. Changes in urban mean temperature and minimum temperature are found to be statistically significant, and can be explained by changes in surface thermal properties such as heat capacity and thermal conductivity. This explanation is supported by figure 5 which shows the diurnal energy cycle averaged over the regions that are transformed from native vegetation in 2005 to urban in 2050 (newly urbanized). Transforming the natural land surface to urbanized results in more energy being stored as ground heat flux during the daytime from 7 am to 4 pm local time, whereas more positive ground heat flux appears during the night indicate more energy being released (warming the atmosphere) and leading to warmer air temperatures.

At the same time, urbanization results in decreased latent heat flux throughout the day, and the reduced evaporation limits the availability of atmospheric column water for convective processes. This result is similar to the findings of Georgescu et al. (2012). Meanwhile, our results show that greater sensible heat flux difference is positive during the night as expected, causing urban nighttime air temperatures to be larger. However, daytime sensible heat flux differences are negative. This, somewhat surprising result agrees with previous findings (Cao and Lin 2014), and can be attributed to the decrease in turbulent activity associated with the canyons of the urban canopy scheme. The vertical wind speed profile in the UCM follows that in previous literature Swaid (1993), with in-canyon wind speed being exponentially proportional to the wind speed above the canyon, and helping to determine the heat flux exchange between the canyon wall, street and the air. When canyon wind speed is reduced due to the canyon structure following the exponential relation, the sensible heat flux from the wall and street to canyon is reduced as well, as reflected by the reduced sensible heat flux.

The diurnal temperature variation over the newly urbanized areas is also shown in figure 5. The magnitude of difference in maximum and minimum temperature is consistent with the previous analysis. However the occurrence of maximum and minimum temperatures are delayed by about 1 hour and 30 minutes respectively. This means a longer duration of higher temperature during the day for LULC_2050, potentially leading to stress for the population residing in the urban areas.

The spatial pattern of sensible and latent heat flux is shown in figure s1 in supplemental file. Sensible heat flux is larger in the western part of the domain (in the lower desert), and smaller in the northeast (higher elevations). In contrast, latent heat flux is greatest in the northeastern mountains and gradually decreases toward the western desert. The differences in the mean sensible heat flux due to urbanization indicates an increase in sensible heat flux (and decrease in latent heat flux) over Tucson and surroundings and the northeast high mountains, indicating a change in the partitioning of available energy. While increased sensible heat flux can indicate less stable conditions that could lead to increased precipitation, the reduced evapotranspiration results in less water available for convection; i.e., the two processes act in opposite directions. As we will show below, decrease in moisture availability leads to less precipitation.

3.3 Urban impacts on precipitation

3.3.1 Urban impacts on summer mean precipitation

Figure 6 shows the 10-year average summertime precipitation difference between LULC_2005 and LULC_2050. A pattern of decreasing precipitation dominates the northeastern mountainous part of the domain and some parts of the urban corridor. A student t test of the difference in daily mean precipitation at each grid cell suggests that this change is statistically significant. However the bootstrap test does not indicate a statistically significantly change, and so the results must be considered to be inconclusive.

Focusing on the diurnal cycle of precipitation, we analyze the precipitation differences for newly urbanized regions (figure 7). The results indicate that while the timing of the peak in the diurnal cycle remains unchanged, there is a marked decrease precipitation (about 6%) during the late afternoon and early evening (1400 – 2100 LST). This suggests reduced precipitation in the newly urbanized areas likely due to reduced evapotranspiration.

To explain the fact that precipitation decreases over the northeastern part of the domain and parts of the urban corridor, we hypothesize that urbanization leads to a decrease in evapotranspiration (figure s1), so that less moisture is available to precipitate in the mountainous areas via regional precipitation recycling (similar to the suggestion by Georgescu et al. 2009b, 2012). It is important to point out, however, that monsoonal precipitation in the southwest US is highly variable both in terms of location and intensity. Figure s2 (in supplemental file) shows the monsoon seasonal (July and August) accumulated precipitation for

each year, from which it is clear that precipitation does not show a consistent pattern within the model domain for this 10-year timespan. Therefore, even if downwind precipitation is indeed changed due to urbanization, the small differences in location of precipitation from year to year would show up as negligible changes when averaging over time. Add to this the fact that different patterns of precipitation are associated with different dominant wind directions, and any signal can disappear simply due to changes in wind direction.

To dig further into this, we further characterized precipitation based on predominant wind patterns. Previous research defines the relative upwind and downwind region based on seasonal or annual dominant wind (Burian and Shepherd 2005; Georgescu et al. 2008; Shepherd 2006). However, moisture sources over the North American Monsoon (NAM) region vary daily. Moisture may come from Gulf of Mexico, the Pacific Ocean, the Gulf of California as well as terrestrial recycling from the Monsoon region (Hu and Dominguez 2014). Different sources of moisture are characterized by different synoptic conditions, and have different associated upwind and downwind regions. We therefore defined 8 flow regimes based on the hourly wind direction at 500 hPa. If the wind direction in more than 50% of the urban area (in 2050) was coming from a particular direction, then that hour was assigned that particular wind direction. We compared the vertically integrated moisture flux to the wind at the 700 hPa and 500 hPa levels, and results indicate that the direction of the wind at 500 hPa level is more similar to the direction of the vertically integrated moisture flux.

Figure 7 shows the accumulated precipitation differences for different wind regimes. While the way to define wind flow regime is subjective, we checked the number of hours that fall into each category and found that (in total) more than 80% of simulated time steps fall in one of the 8 categories, during the remaining 20% of the time steps, the wind direction is spatially variable and does not fall into any category. The most frequent wind directions are southeasterly, southerly and southwesterly, accounting for 64% of all time steps. The least frequent wind patterns are northerly and northwesterly, accounting for less than 5% of the entire simulation period. This result agrees with previous studies analyzing wind flow patterns and the corresponding moisture sources during the monsoon season (Hu and Dominguez 2014). The results show high spatial heterogeneity with regions of increasing precipitation and regions of decreasing precipitation. The decrease in precipitation seen in the mean (figure 6b) seems to arise due to precipitation differences when the wind comes from the southeast and the south, but again, the results are noisy and not statistically significant (see figure s3 in supplemental

file). Even when analyzed based on the dominant flow conditions, the results remain inconclusive.

3.3.2 Urban Impacts on Precipitation Occurrences

Previous research suggests that urban regions may initiate convection (Balling and Brazel 1987; Changnon and Westcott 2002; Takahashi 2003), and hence it is reasonable to expect a larger number of convective days in urban regions, as compared to the native land cover. Here we define a precipitation day when more than 0.1 mm/day of precipitation falls over 20% or more of the urban area in one day. However, these area and precipitation thresholds are subjective, so we tested different thresholds of precipitation and areal cover. Depending on whether the day is designated as a precipitation (p) or not (n) in the current (c) and future (f) land cover experiments, we have 4 possible categories: 1) rains in both LULC_2005 and LULC_2050, (cpfp), 2) no rain in LULC_2005 and rains in LULC_2050, (cnfp), 3) rains in LULC_2005 and no rain in LULC_2050, (cpfn), 4) doesn't rain in either, (cnfn). Precipitation days each of the 4 categories are shown in Table 1. By comparing cnfp and cpfn, we can determine whether more precipitation days occur due to urbanization. As expected in an arid region, most days are "not precipitation" days in both LULC scenarios. When looking at the other cases, our results suggest a reduction in precipitation days due to urbanization (6 out of 9 cases), however, the results depend on the precipitation and areal cover thresholds used.

3.4 Urban impacts on water and energy demand

Our results suggest that projected expansion of the urban corridor in the Phoenix-Tucson area (as simulated by WRF) may affect both temperature and precipitation, which can be expected to affect water and energy demand in the region. The Arizona Department of Water Resources (ADWR) provides water demand information and assessments for each active management area (i.e., area that heavily relies on the groundwater supply). The goal is to ensure that, by the year 2025, groundwater be withdrawn at a rate that equals the recharge. Tucson and Phoenix are located in the Tucson Active Management Area (i.e. TAMA) and Phoenix Active Management Area (PAMA), respectively. Historically, Tucson municipal water demand has increased by 68% from 1.39×10^{8} m^3 yr^{-1} in 1985 to 2.33×10^{8} m^3 yr^{-1} in 2006. During the same period, Phoenix municipal water demand grew by 76%, increasing from 7.82×10^{8} m^3 to 1.38×10^{9} m^3 per year. The total water demand increase for both cities was roughly 75%. At the

same time, Tucson's area grew by 124% and Phoenix's area grew by 50% - the area of the two cities combined grew by 68%. This indicates that during this period, the water demand for the two cities combined grew almost linearly with area (with Tucson growing more but conserving more water per area than Phoenix). Based on these estimates, the land use projections used in this study (that urban extent in 2050 is about 7 times larger than in 2005), and an assumption that water usage intensity remains the same in year 2050 as in 2005, we estimate that water demand will grow (linearly) to around 1.12×10^{10} m^3 for the entire corridor. Bear in mind that this urban projection is made by assuming a scenario of high rates urban expansion, and it is not likely that this water demand will be easily satisfied, especially given the water-limited nature of the State of Arizona.

Groundwater is an important water source in the State of Arizona, accounting for 64% of water supply in TAMA and 31% in PAMA in 2006. The ADWR projections of future water demand are based on population growth rate and water use, with the assumption that when the full utilization of all other water sources cannot meet the demand, groundwater can be utilized to meet the remainder. In their highest water demand scenario, municipal water demands are 3.80×10^{8} m^3 and 2.59×10^{9} m^3 for TAMA and PAMA respectively, requiring groundwater overdrafts in 2025. Our estimates indicate a much larger water demand by 2050 (under the assumptions stated above), suggesting there will simply not be enough water to sustain that level of urbanization. Thus, urban growth to the extent portrayed by LULC_2050 is probably unsustainable, with water being an important limitation to future urbanization unless alternative sources are found.

Meanwhile, temperature increases within the urban area (along with the greenhouse gas-induced global climate change) are likely to increase energy demands for electricity cooling needs (Georgescu et al. 2013). Cooling demands in the urban areas are known to account for more than 50% of the total electricity demand, with this ratio climbing to as high as 65% during the hot season evening hours in semi-arid urban environments (Salamanca et al. 2013). Here we use electric load data for Tucson and Phoenix and assume the ratio of air conditioning (AC) consumption to total electric load as following the diurnal pattern as shown in Salamanca et al., 2013. The data are provided at the intra-daily timescale by Tucson Electric Power for Tucson and Arizona Public Service (APS) and Salt River Project (SRP) for Phoenix. The diurnal AC consumption in each city is obtained by multiplying the diurnal total electric load to the corrected

ratio. Figure 9 shows that the AC consumption follows a very similar diurnal pattern to the diurnal temperature observed within the urban area for the same period.

To project AC consumption under warmer temperatures, temperature and electric load were fitted to a polynomial function (with linear correlation coefficient of 0.85 for Tucson and 0.85 for Phoenix); the results clearly suggest that temperature plays a significant role in influencing the AC consumption (see figure 10). Then for each hour during the day, the increased energy load due to UHI-induced temperature increase can be obtained from the fitted function. Consequently, the projected future total AC consumption accounts for increase in temperature as well as the urban expansion. Even though there are many other factors that may affect the energy consumption, it is safe to assume that areal enlargement and temperature are likely to be among the most important factors affecting future AC consumption. Considering larger area and temperature simultaneously, the projection of future additional AC consumption demand for Tucson and Phoenix is shown in figure 11. Overall, the areal enlargement due to urban expansion appears to be the dominant factor affecting energy consumption in the future.

4. CONCLUSIONS

This study has examined the climatological effects associated with potential expansion of the Phoenix-Tucson urban corridor on summer monsoonal (July and August) climate in Arizona. It needs to be emphasized that only the impact of urbanization is studied here, while the expected global warming effect from 1991 to 2050 is not considered. Given that the Phoenix metropolitan area has been one the most rapidly developing areas in the United States during the past 30 years, and that the Phoenix-Tucson 'Sun' Corridor is still expected to add another 5 to 6 million inhabitants from 2000 to 2030 (US Census, 2005), it is useful for planners to understand how urbanization can affect the hydroclimate of the region. We used high-resolution simulations of 10 monsoon seasons (from 1991 to 2000) generated by the WRF model under a current representation of land cover (LULC_2005) and a projected land cover representative of high rates of urban expansion (LULC_2050).

Our results suggest that urbanization will likely not impact the magnitudes of daily maximum temperatures, but may result in significant increases in daily minimum (night time) temperatures over the urban corridor. This agrees with previous research indicating that the urban heat island is mainly a nocturnal phenomenon. Accordingly the increases in daily mean temperature are mainly due to increased nighttime temperatures. These results agree with Georgescu et al., (2013). However, both the daily maximum and minimum temperature are delayed, with about an hour for the maximum and 30 minutes for the minimum temperatures resulting in longer periods of hotter temperatures. Such increased temperatures will likely increase the risk of heat related health issues and even death (McGeehin and Mirabelli 2001). Of course, it is possible that implementation of 'cool-roof' technology could help to reduce the UHI phenomenon providing a potential solution to relieve the impact on temperature (Georgescu et al. 2013).

Surprisingly, our energy diurnal cycles over the newly urbanized region suggest that sensible heat flux will increase during the nighttime and decrease during the day (due to sensible heat flux calculations in the urban canopy model, as explained earlier). Meanwhile latent heat fluxes are likely to decrease dramatically throughout the day, resulting in less evaporation over urban regions and downwind mountainous areas. The overall effect of urbanization is likely to be less moisture available for convection. Overall, our results indicate that the ground heat flux difference will be negative during the day and positive during the night, indicating energy storage within the soil column during the day and release to the atmosphere during the night.

We also examined the potential changes in 10-year climatological summertime precipitation due to urbanization. Statistical significant decreases in precipitation can be expected over the mountains at higher elevations in the northern parts of the domain and parts of the newly urbanized region. Meanwhile the simulations indicate decreased evening precipitation in the newly urbanized region. However, an analysis based on dominant wind direction did not provide statistical significant evidence for changes in precipitation patterns. These results are consistent with those of Georgescu et al. 2012. However, unlike Georgescu et al. 2012, our results are much more spatially heterogeneous (a result of using very high resolution to conduct the simulations) and reductions are only seen in the mountainous northeastern part of the domain and part of the urbanized region.

Overall, while our temperature results appear to be robust, our precipitation results must be treated as inconclusive. Due to the complex nature of convective precipitation in the southwest US, each precipitation event has its unique intensity and location. Consequently, precipitation changes over the downwind region will likely not result in robust changes to spatial patterns. While this problem might potentially be solved by use of a larger sample size, it seems unlikely. We hypothesize that because the ambient air is very dry, impacts of urbanization on energy partitioning at the surface will not result in significant changes in precipitation because there is simply not enough available specific humidity. In contrast, similar research conducted in Tokyo, Japan, where summertime relative humidity is usually above 70%, reported increased precipitation over the metropolitan area (Kusaka et al. 2014).

Finally, we developed rough estimates of future water and energy demand based on urban expansion and temperature change. Assuming that increase in urban area is the main factor influencing the water demand, our estimates indicate that about 7 times the current water supply would be needed to sustain an urban scale like LULC_2050, which would requires extensive access to groundwater storage. This suggests that projected urban expansion to the extent represented by LULC_2050 will be very difficult to achieve without access to new sources of water. Meanwhile, energy supplies will have to be expanded to meet future air conditioning needs to deal with the longer durations of high day and nighttime temperatures.

There are, of course, limitations to our study that must be accounted for in any analysis involving urban planning. In particular, we did not consider the impacts of aerosol, even though the role of aerosols in urban environments will likely be an important factor. Other limitations

include the lack of consideration of irrigation effects in the land surface representation, which can be expected to have a significant impact on the water and energy budget over the region. Irrigation over urban areas can actually increase the latent heat flux while decreasing the sensible heat flux, leads to the so-called “oasis” effect (Georgescu et al. 2011) and potentially contributing to changes in precipitation. It is important to emphasize that our study does not include urban irrigation, which could be important in cities like Phoenix and Tucson. To evaluate the potential impact of urban irrigation in our results, we performed a sensitivity study with a rough characterization of urban irrigation where soil moisture was set to saturation over 15% of the urban area. Our results show that with-and without urban irrigation, temperature increases over the newly urbanized region and precipitation decreases over the entire domain and in particular over the newly urbanized region. While including urban irrigation generates a weaker response (there is more precipitation in the urban irrigation case), there is still an overall decrease in precipitation due to increased urbanization. Another important factor affecting regional precipitation may be precipitation recycling (Georgescu et al. 2009b). Studies exploring these and other effects will be reported in future papers.

Acknowledgements: This work was supported by the EU-funded project ‘Sustainable Water Action (SWAN): Building Research Links Between EU and US’ (INCO-20011-7.6 grant number 294947). We thank APS, TEP and SRP for providing electric load data.

5. REFERENCES

Baik, J. J., Y. H. Kim, and H. Y. Chun, 2001: Dry and moist convection forced by an urban heat island. *Journal of Applied Meteorology*, **40,** 1462-1475.

Balling, R. C., and S. W. Brazel, 1987: Recent Changes in Phoenix, Arizona Summertime Diurnal Precipitation Patterns. *Theor Appl Climatol*, **38,** 50-54.

Brazel, A., P. Gober, S. J. Lee, S. Grossman-Clarke, J. Zehnder, B. Hedquist, and E. Comparri, 2007: Determinants of changes in the regional urban heat island in metropolitan Phoenix (Arizona, USA) between 1990 and 2004. *Climate Research*, **33,** 171-182.

Burian, S. J., and J. M. Shepherd, 2005: Effect of urbanization on the diurnal rainfall pattern in Houston. *Hydrol Process*, **19,** 1089-1103.

Cao, M., and Z. Lin, 2014: Impact of Urban Surface Roughness Length Parameterization Scheme on Urban Atmospheric Environment Simulation. *Journal of Applied Mathematics*, **2014,** 14.

Changnon, S. A., 1979: Rainfall changes in summer caused by St. Louis. *Science*, **205,** 402-404.

——, 1980: More on the La Porte Anomaly: A Review. *Bulletin of the American Meteorological Society*, **61,** 702-711.

——, and N. E. Westcott, 2002: Heavy rainstorms in Chicago: Increasing frequency, altered impacts, and future implications. *J Am Water Resour As*, **38,** 1467-1475.

——, F. A. Huff, P. T. Schickedanz, and J. L. Vogel, 1977: Summary of METROMEX, volume 1: weather anomalies and impacts.

——, R. G. Semonin, A. H. Auer, R. R. Braham, and J. Hales, 1981: METROMEX: A Review and Summary. Meteor. Monogr.

Chen, F., and J. Dudhia, 2001: Coupling an advanced land surface-hydrology model with the Penn State-NCAR MM5 modeling system. Part I: Model implementation and sensitivity. *Monthly Weather Review*, **129,** 569-585.

Chow, W. T. L., D. Brennan, and A. J. Brazel, 2012: Urban Heat Island Research in Phoenix, Arizona Theoretical Contributions and Policy Applications. *Bulletin of the American Meteorological Society*, **93,** 517-530.

Climte Central, 2014: Summer in the City: Hot and Getting Hotter. Available at http://assets.climatecentral.org/pdfs/UrbanHeatIsland.pdf

Collins, W. D., and Coauthors, 2004: Description of the NCAR community atmosphere model (CAM 3.0).

Commission for Environmental Cooperation. 2013. 2005 North American Land Cover at 250 m spatial resolution. Produced by Natural Resources Canada/Canadian Center for Remote Sensing (NRCan/CCRS), United States Geological Survey (USGS); Insituto Nacional de Estadística y Geografía (INEGI), Comisión Nacional para el Conocimiento y Uso de la Biodiversidad (CONABIO) and Comisión Nacional Forestal (CONAFOR). Available at http://www.cec.org/naatlas/

Craig, K., and R. Bornstein, 2002: MM5 Simulations of urban induced convective precipitation over Atlanta, GA, San Jose State University.

Georgescu, M., A. Mahalov, and M. Moustaoui, 2012: Seasonal hydroclimatic impacts of Sun Corridor expansion. *Environ Res Lett*, **7**.

——, G. Miguez-Macho, L. T. Steyaert, and C. P. Weaver, 2008: Sensitivity of summer climate to anthropogenic land-cover change over the Greater Phoenix, AZ, region. *J Arid Environ*, **72,** 1358-1373.

——, 2009a: Climatic effects of 30 years of landscape change over the Greater Phoenix, Arizona, region: 1. Surface energy budget changes. *J Geophys Res-Atmos*, **114**.

——, 2009b: Climatic effects of 30 years of landscape change over the Greater Phoenix, Arizona, region: 2. Dynamical and thermodynamical response. *J Geophys Res-Atmos*, **114**.

——, M. Moustaoui, A. Mahalov, and J. Dudhia, 2011: An alternative explanation of the semiarid urban area "oasis effect". *J Geophys Res-Atmos*, **116**.

——, 2013: Summer-time climate impacts of projected megapolitan expansion in Arizona. *Nat Clim Change*, **3,** 37-41.

Hu, H., and F. Dominguez, 2014: Evaluation of Oceanic and Terrestrial Sources of Moisture for the North American Monsoon Using Numerical Models and Precipitation Stable Isotopes. *Journal of Hydrometeorology*, **16,** 19-35.

Huff, F. A., and J. L. Vogel, 1978: Urban, topographic and diurnal effects on rainfall in the St. Louis region. *Journal of Applied Meteorology*, **17,** 565-577.

Janjić, Z. I., 1990: The step-mountain coordinate: Physical package. *Monthly Weather Review*, **118,** 1429-1443.

——, 1996: The surface layer parameterization in the NCEP Eta Model. *WORLD METEOROLOGICAL ORGANIZATION-PUBLICATIONS-WMO TD***,** 4.16-14.17.

——, 2002: Nonsingular implementation of the Mellor–Yamada level 2.5 scheme in the NCEP Meso model. *NCEP office note*, **437,** 61.

Kain, J. S., 2004: The Kain-Fritsch convective parameterization: An update. *Journal of Applied Meteorology*, **43,** 170-181.

Kaufmann, R. K., K. C. Seto, A. Schneider, Z. Liu, L. Zhou, and W. Wang, 2007: Climate Response to Rapid Urban Growth: Evidence of a Human-Induced Precipitation Deficit. *Journal of Climate*, **20,** 2299-2306.

Kusaka, H., and F. Kimura, 2004: Coupling a single-layer urban canopy model with a simple atmospheric model: Impact on urban heat island simulation for an idealized case. *J Meteorol Soc Jpn*, **82,** 67-80.

——, H. Kondo, Y. Kikegawa, and F. Kimura, 2001: A simple single-layer urban canopy model for atmospheric models: Comparison with multi-layer and slab models. *Bound-Lay Meteorol*, **101,** 329-358.

——, K. Nawata, A. Suzuki-Parker, Y. Takane, and N. Furuhashi, 2014: Mechanism of Precipitation Increase with Urbanization in Tokyo as Revealed by Ensemble Climate Simulations. *J Appl Meteorol Clim*, **53,** 824-839.

Lin, C. Y., W. C. Chen, P. L. Chang, and Y. F. Sheng, 2011: Impact of the Urban Heat Island Effect on Precipitation over a Complex Geographic Environment in Northern Taiwan. *J Appl Meteorol Clim*, **50,** 339-353.

Maricopa Association of Governments. 2005. Arizona Growth Maps and Algorithm. Unpublished report.

McGeehin, M. A., and M. Mirabelli, 2001: The potential impacts of climate variability and change on temperature-related morbidity and mortality in the United States. *Environmental Health Perspectives*, **109,** 185-189.

Mellor, G. L., and T. Yamada, 1982: Development of a turbulence closure model for geophysical fluid problems. *Reviews of Geophysics*, **20,** 851-875.

Mesinger, F., and Coauthors, 2006: North American regional reanalysis. *Bulletin of the American Meteorological Society*, **87,** 343-+.

Morrison, H., G. Thompson, and V. Tatarskii, 2009: Impact of Cloud Microphysics on the Development of Trailing Stratiform Precipitation in a Simulated Squall Line: Comparison of One- and Two-Moment Schemes. *Monthly Weather Review*, **137,** 991-1007.

Norman, L. M., M. Feller, and M. L. Villarreal, 2012: Developing spatially explicit footprints of plausible land-use scenarios in the Santa Cruz Watershed, Arizona and Sonora. Landscape Urban Plan, **107**, 225-235.

Salamanca, F., M. Georgescu, A. Mahalov, M. Moustaoui, M. Wang, and B. M. Svoma, 2013: Assessing summertime urban air conditioning consumption in a semiarid environment. *Environ Res Lett*, **8**.

Shepherd, J. M., 2005: A Review of Current Investigations of Urban-Induced Rainfall and Recommendations for the Future. *Earth Interactions*, **9,** 1-27.

——, 2006: Evidence of urban-induced precipitation variability in arid climate regimes. *J Arid Environ*, **67,** 607-628.

Skamarock, W., and Coauthors, 2008: A description of the advanced research WRF version 3. *NCAR technical note NCAR/TN/u2013475*.

Svoma, B. M., and A. Brazel, 2010: Urban effects on the diurnal temperature cycle in Phoenix, Arizona. Climate Research, **41**, 21-29.

Swaid, H., 1993: The role of radiative-convective interaction in creating the microclimate of urban street canyons. *Bound-Lay Meteorol*, **64,** 231-259.

Takahashi, H., 2003: Secular variation in the occurrence property of summertime daily rainfall amount in and around the Tokyo Metropolitan area. *Tenki*, **50,** 31-41.

Tayanç, M., M. Karaca, and O. Yenigün, 1997: Annual and seasonal air temperature trend patterns of climate change and urbanization effects in relation to air pollutants in Turkey. *Journal of Geophysical Research: Atmospheres (1984–2012)*, **102,** 1909-1919.

Tewari, M., F. Chen, and H. Kusaka, 2006: Implementation and evaluation of a single-layer urban canopy model in WRF/Noah. *WRF users workshop 2006*.

US Census Bureau, 2005: Population Division Interim State Population Projections.

——, 2010: Population Division Interim State Population Projections.

Veerbeek, W., H. Denekew, A. Pathirana, D. Brdjanovic, C. Zevenbergen, and T. K. Bacchin, 2011: Urban growth modeling to predict the changes in the urban microclimate and urban water cycle.

Zoubir, A. M., and B. Boashash, 1998: The bootstrap and its application in signal processing. *Ieee Signal Proc Mag*, **15,** 56-76.

Tables

Table 1: number of days in each category (as discussed in the text) with regard to whether it was convective day or not in each land cover representation.

precipitation threshold (mm/day)	area threshold (%)	cnfn	cpfn	cnfp	cpfp	More Precip. in Future LULC
0.1	20	305	21	23	241	T
0.5	20	367	27	14	182	F
1	20	408	16	14	152	F
0.1	30	370	22	12	186	F
0.5	30	431	11	16	132	T
1	30	459	16	17	98	F
0.1	40	411	18	15	146	F
0.5	40	470	19	13	88	F
1	40	494	11	16	69	T

T indicates that cnfp is greater than cpfn, which means more convective days occur due to urbanization, on the contrary; F indicates less convective days occur due to urbanization.

Figures

Figure Captions

Figure 1: In 2005, Phoenix and Tucson are represented as the red and blue crossed region. The Phoenix-Tucson Corridor in 2050 is represented as the black slash area. Domain 1 and 2 are represented as the black dash and red box. Elevations are shown in meter.

Figure 2: On the left, 10-year summertime (July and August) mean temperature (in ˚C) from a) WRF simulated, c) PRISM, e) NARR data ; On the right, 10-year July and August mean precipitation from b) WRF, d) PRISM , f) NARR data.

Figure 3: Domain averaged July and August accumulated precipitation variation in WRF, PRISM and NARR from 1991 to 2000 (upper). Domain averaged July and August domain average temperature variation in WRF, PRISM, and NARR from 1991 and 2000 (bottom).

Figure 4: July and August simulated temperature difference between LULC_2050 and LULC_2005, a) mean temperature in LULC_2005, b) mean temperature difference between LULC_2050 and LULC_2005, c) student t test and bootstrap test for mean temperature difference, orange (blue) indicates significant increase (decrease) in both statistical tests, d), e) and f) are similar to a), b) and c) except for maximum temperature, g), h) and 1) are similar to a), b) and c) except for minimum temperature.

Figure 5: On the upper, energy diurnal cycle over the newly urbanized area, including sensible heat flux (SH), latent heat flux (LH), ground heat flux (GRD) and net radiation (Net) for LULC_2005(solid line) and LULC_2050 (dash line). On the bottom, temperature diurnal cycle over newly urbanized area for LULC_2005 (solid line) and LULC_2050 (dash line).

Figure 6: a) Average July and August accumulated precipitation from 1991 to 2000 in LULC_2005. b) July and August precipitation difference between LULC_2050 and LULC_2005 from 1991 to 2000, normalized by number of days. c) Bootstrap test of difference in daily precipitation between LULC_2005 and LULC_2050, blue (orange) indicates statistically significant decrease (increase), d) Similar to c) except for student t test, blue indicates statistically significant decrease.

Figure 7: Precipitation difference between LULC_2050 and LULC_2005 under each of the flow regime.

Figure 8: Diurnal cycle of precipitation over the newly urbanized area in LULC_2050 (red) and LULC_2005 (blue).

Figure 9: Diurnal cycle of Air Conditioning (AC) consumption and temperature at Phoenix metropolitan and Tucson metropolitan.

Figure 10: Scatter plot of the AC consumption and temperature data, the green line indicates the fitted polynomial function.

Figure 11: AC consumption of Tucson and Phoenix in 2005 and 2050, considering both areal enlargement and warmer temperature.

Figures

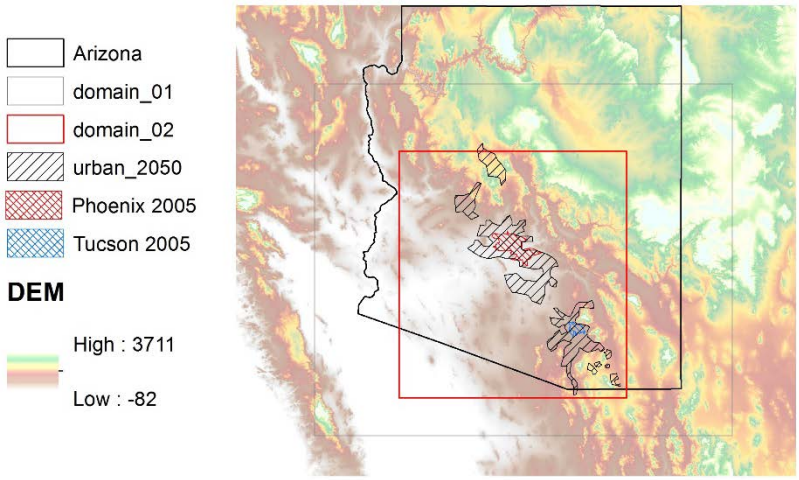

Figure 1: In 2005, Phoenix and Tucson are represented as the red and blue crossed region. The Phoenix-Tucson Corridor in 2050 is represented as the black slash area. Domain 1 and 2 are represented as the black dash and red box. Elevations are shown in meter.

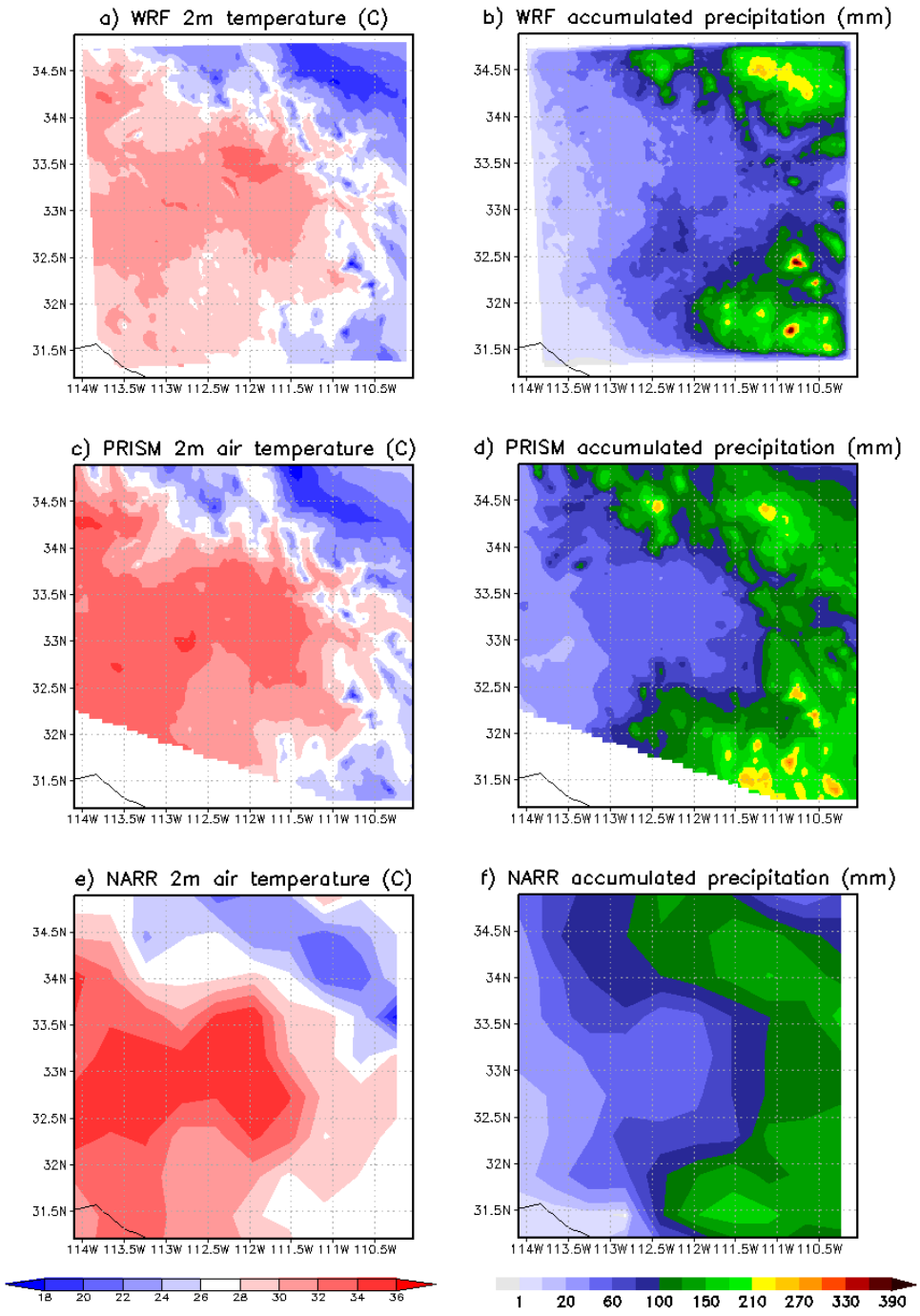

Figure 2: On the left, 10-year July and August mean temperature (in ^{o}C) from a) WRF, c) PRISM, e) NARR data. On the right, 10-year summertime (July and August) mean accumulated precipitation from b) WRF simulated, d) PRISM, f) NARR data.

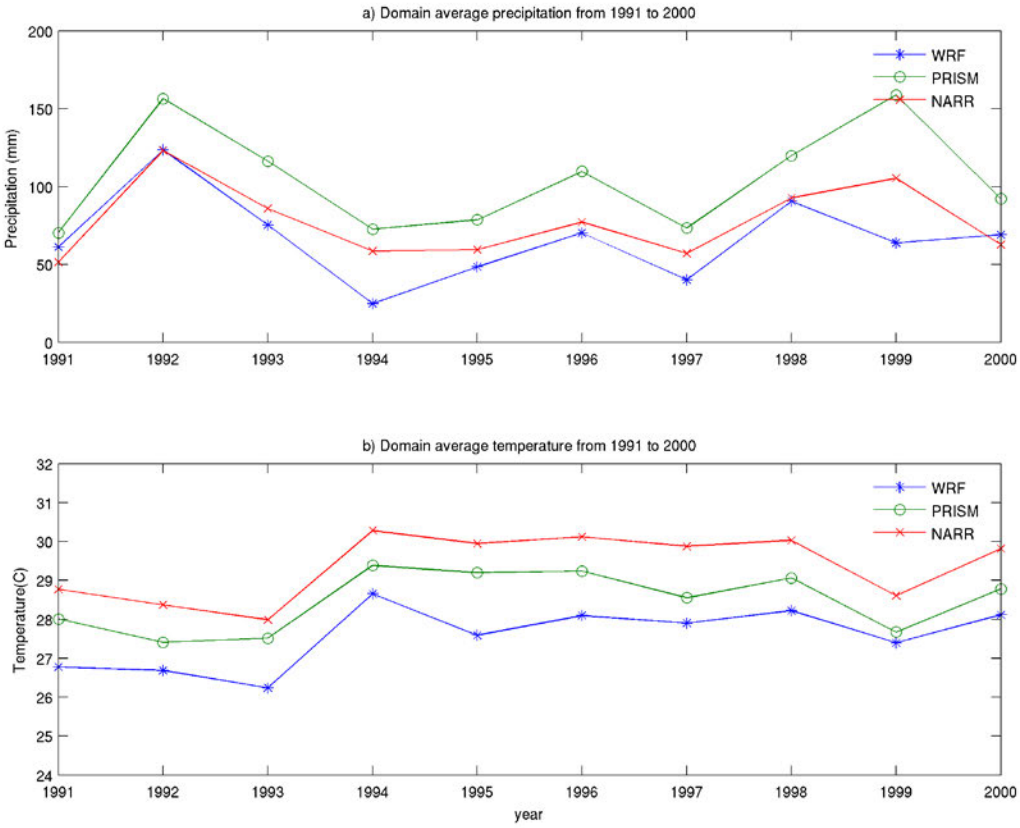

Figure 3: Domain averaged July and August accumulated precipitation variation in WRF, PRISM and NARR from 1991 to 2000 (upper). Domain averaged July and August domain average temperature variation in WRF, PRISM, and NARR from 1991 and 2000 (bottom).

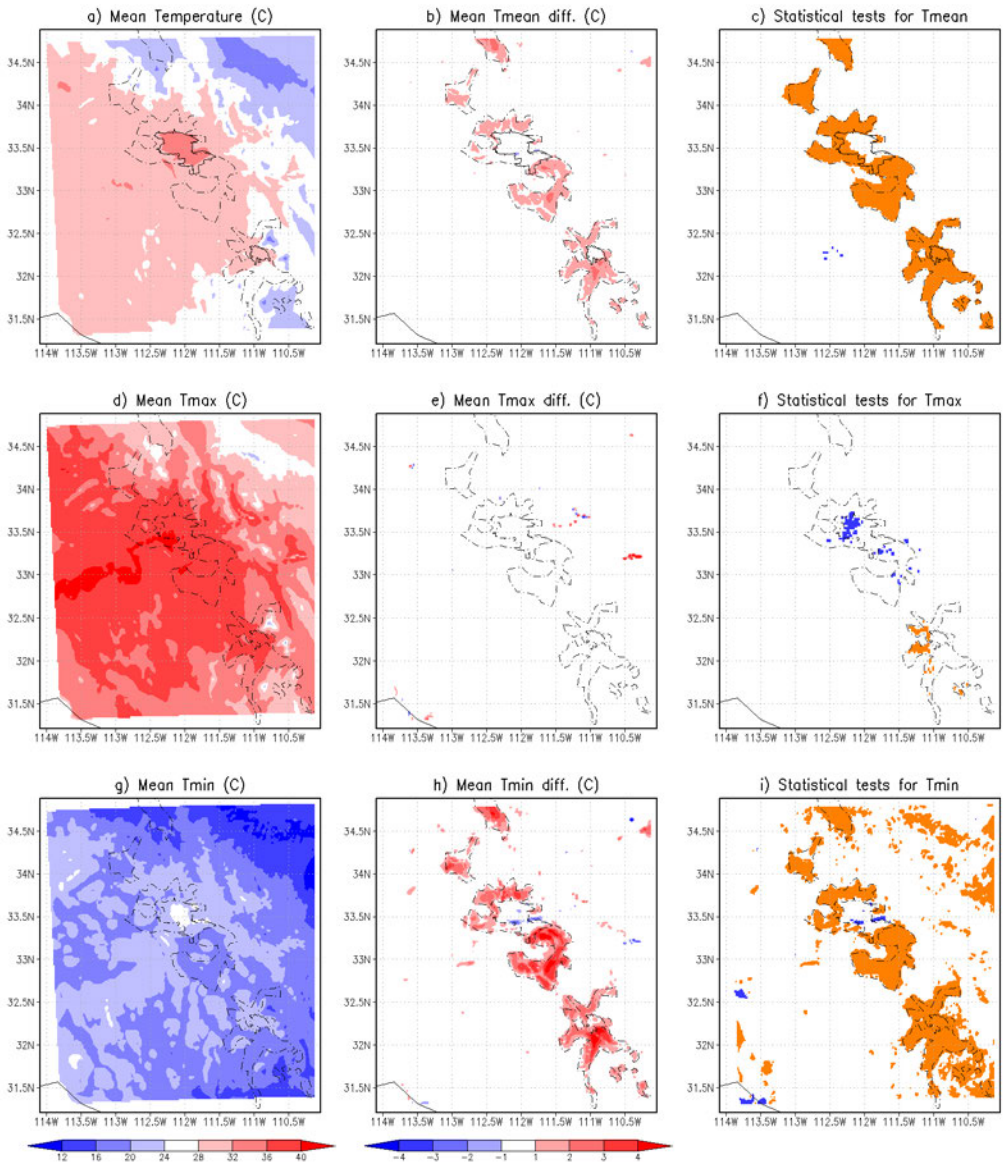

Figure 4: July and August simulated temperature difference between LULC_2050 and LULC_2005, a) mean temperature in LULC_2005, b) mean temperature difference between LULC_2050 and LULC_2005, c) student t test for mean temperature difference, orange (blue) indicates significant increase (decrease), d), e) and f) are similar to a), b) and c) except for maximum temperature, g), h) and 1) are similar to a), b) and c) except for minimum temperature.

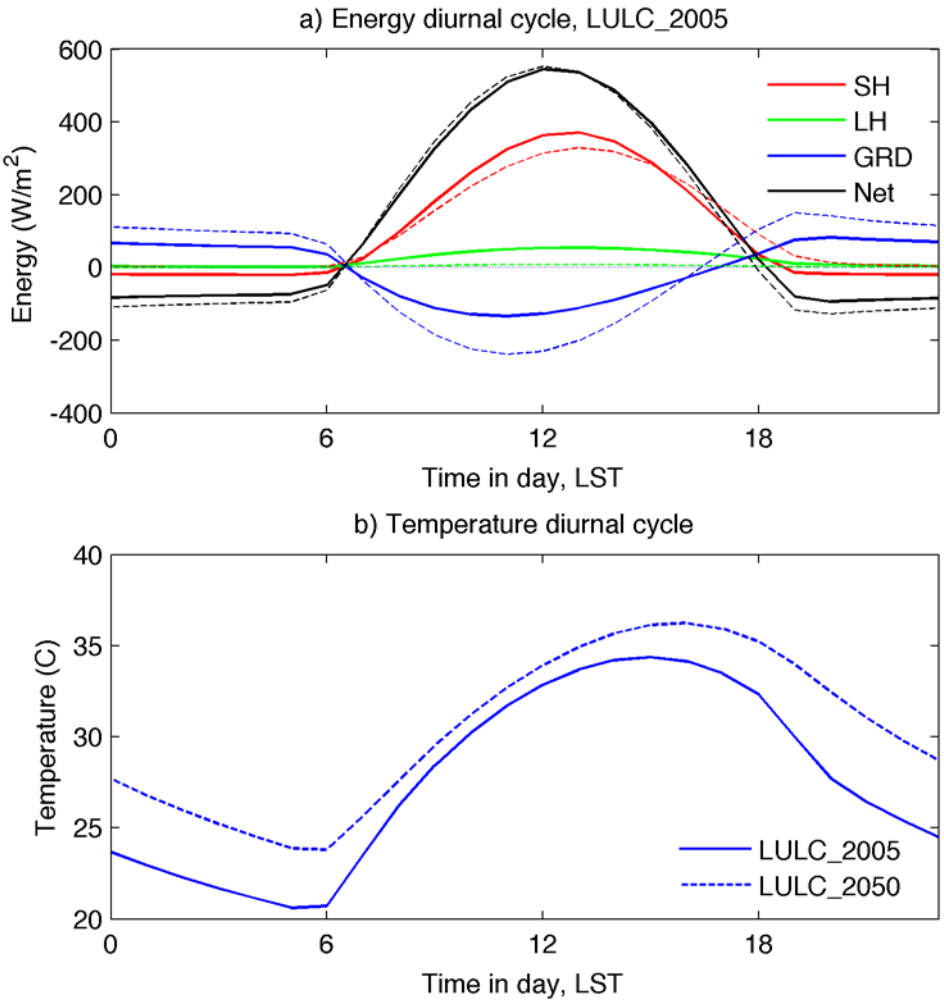

Figure 5: On the upper, energy diurnal cycle over the newly urbanized area, including sensible heat flux (SH), latent heat flux (LH), ground heat flux (GRD) and net radiation (Net) for LULC_2005(solid line) and LULC_2050 (dash line). On the bottom, temperature diurnal cycle over newly urbanized area for LULC_2005 (solid line) and LULC_2050 (dash line).

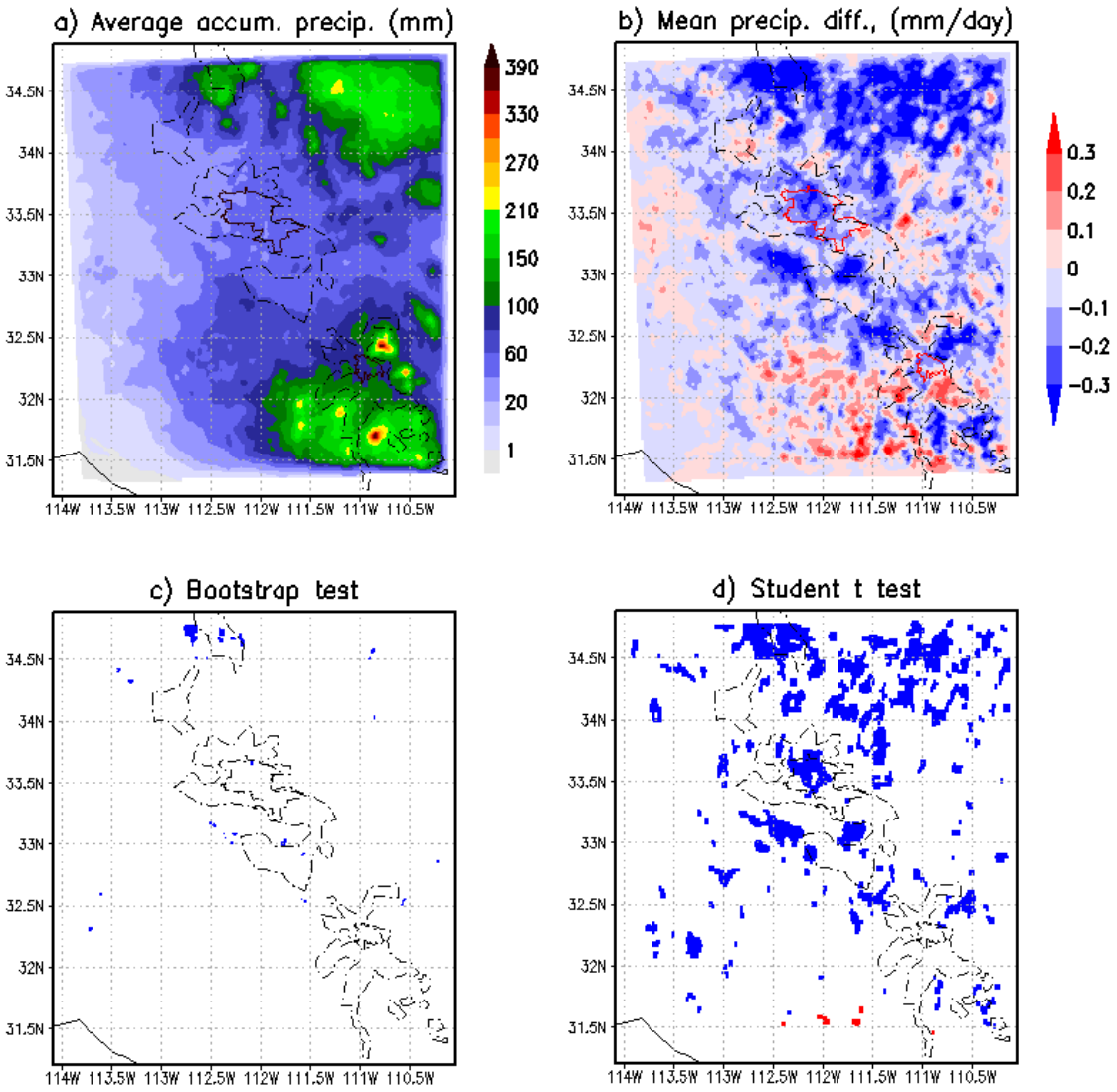

Figure 6: a) Average July and August accumulated precipitation from 1991 to 2000 in LULC_2005. b) July and August precipitation difference between LULC_2050 and LULC_2005 from 1991 to 2000, normalized by number of days. c) Bootstrap test of difference in daily precipitation between LULC_2005 and LULC_2050, blue (orange) indicates statistically significant decrease (increase), d) Similar to c) except for student t test, blue indicates statistically significant decrease.

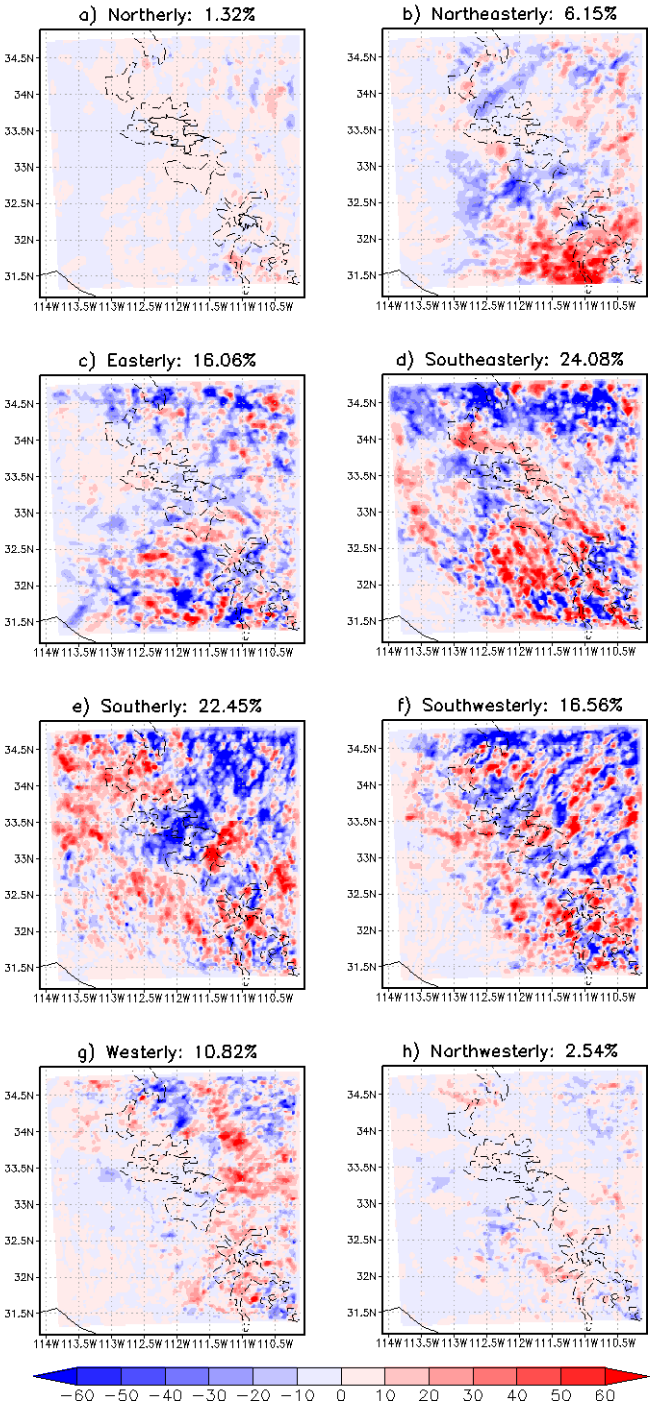

Figure 7: Precipitation difference between LULC_2050 and LULC_2005 under each of the flow regime.

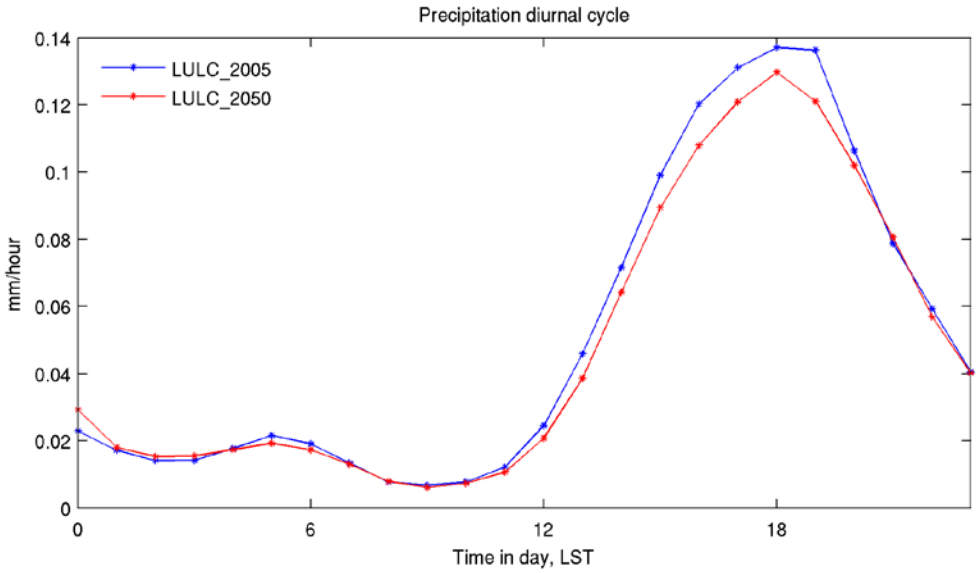

Figure 8: Diurnal cycle of precipitation over the newly urbanized area in LULC_2050 (red) and LULC_2005 (blue).

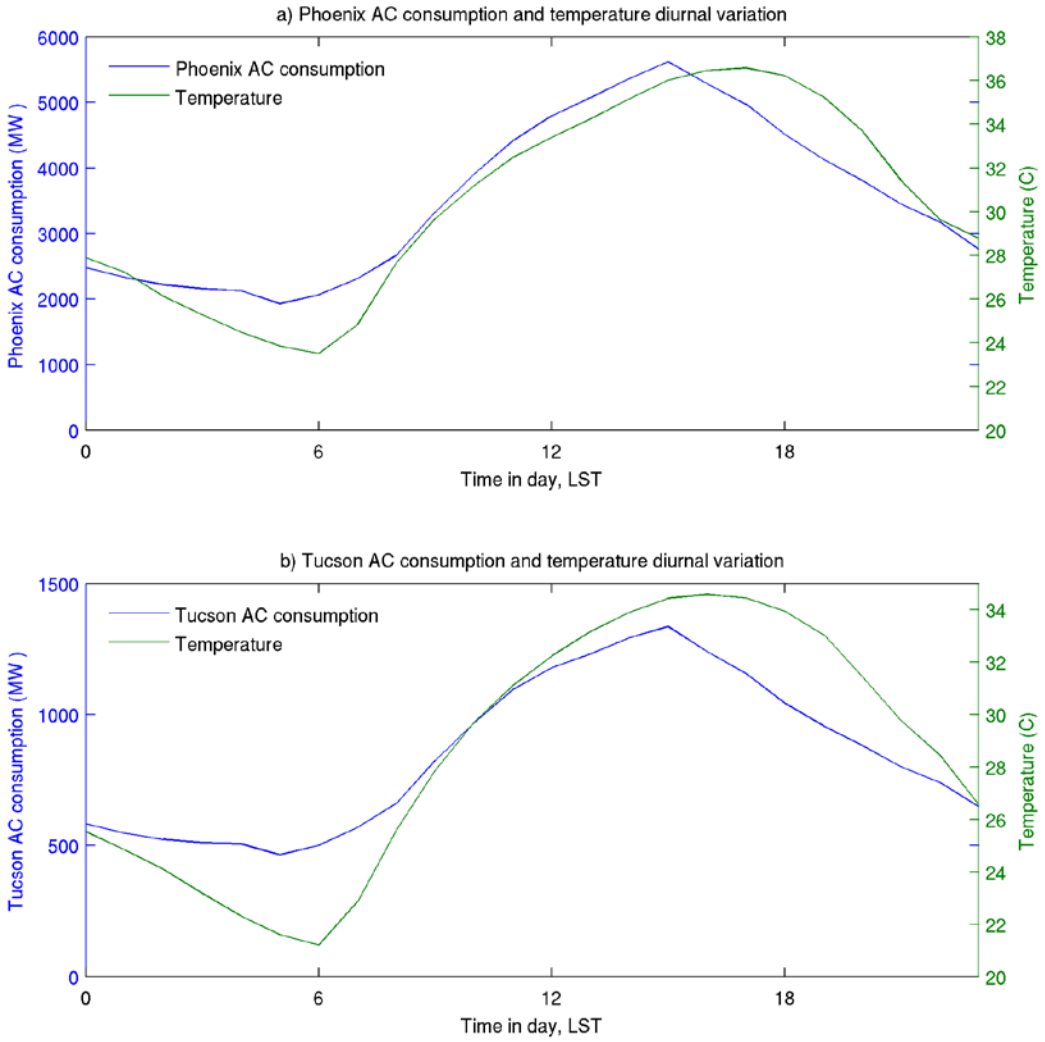

Figure 9: Diurnal cycle of Air Conditioning (AC) consumption and temperature at Phoenix metropolitan and Tucson metropolitan.

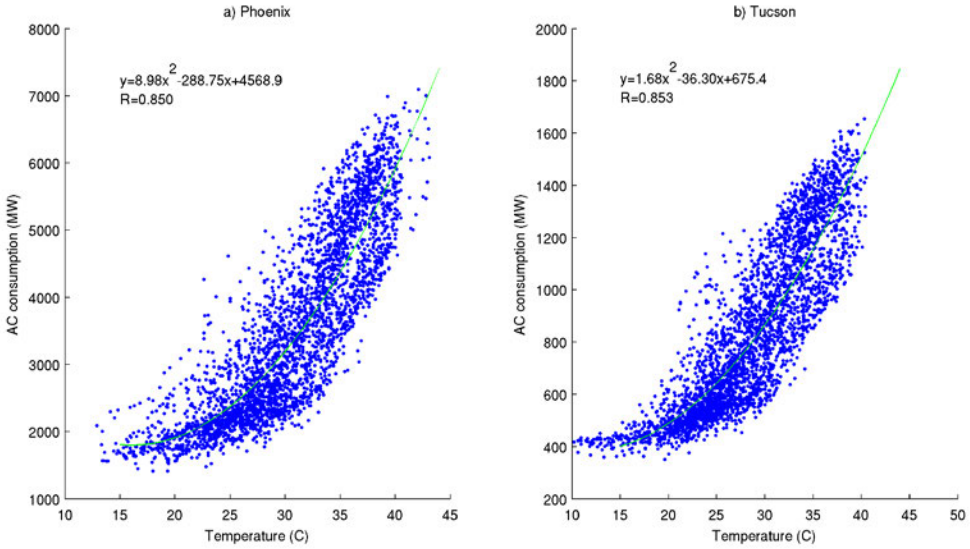

Figure 10: Scatter plot of the AC consumption and temperature data, the green line indicates the fitted polynomial function.

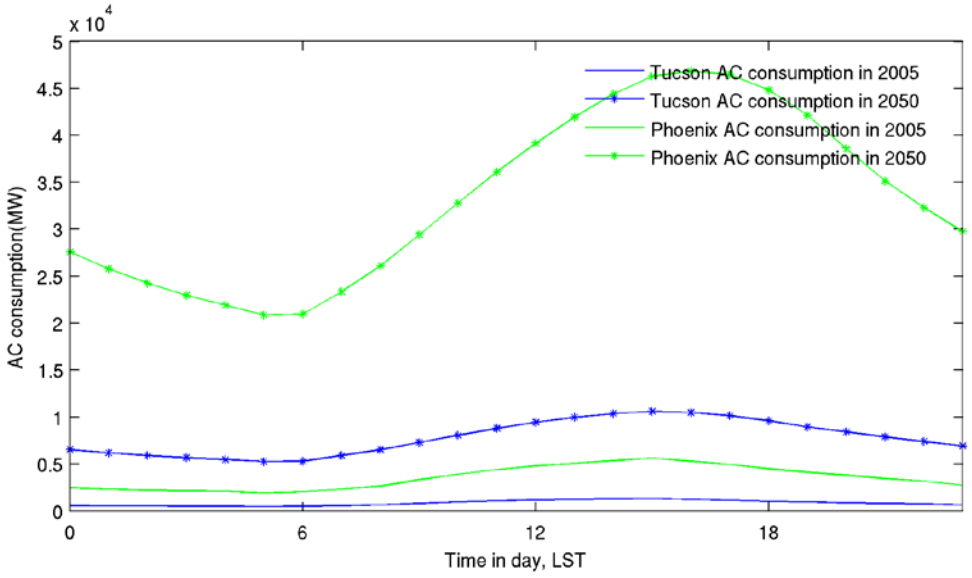

Figure 11: AC consumption of Tucson and Phoenix in 2005 and 2050, considering both areal enlargement and warmer temperature.

Supplemental Materials

Figure s1: a) Average sensible heat flux in July and August from 1991 to 2000 in LULC_2005. b) Average sensible heat flux difference between LULC_2050 and LULC_2005. c) Similar to a) but for latent heat flux. d) Similar to b) but for latent heat flux difference.

Figure s2: Simulated July and August precipitation pattern from 1991 to 2000 with landscape representation LULC_2005.

Figure s3: Difference of mean test for precipitation under each flow regime, no significant pattern observed.

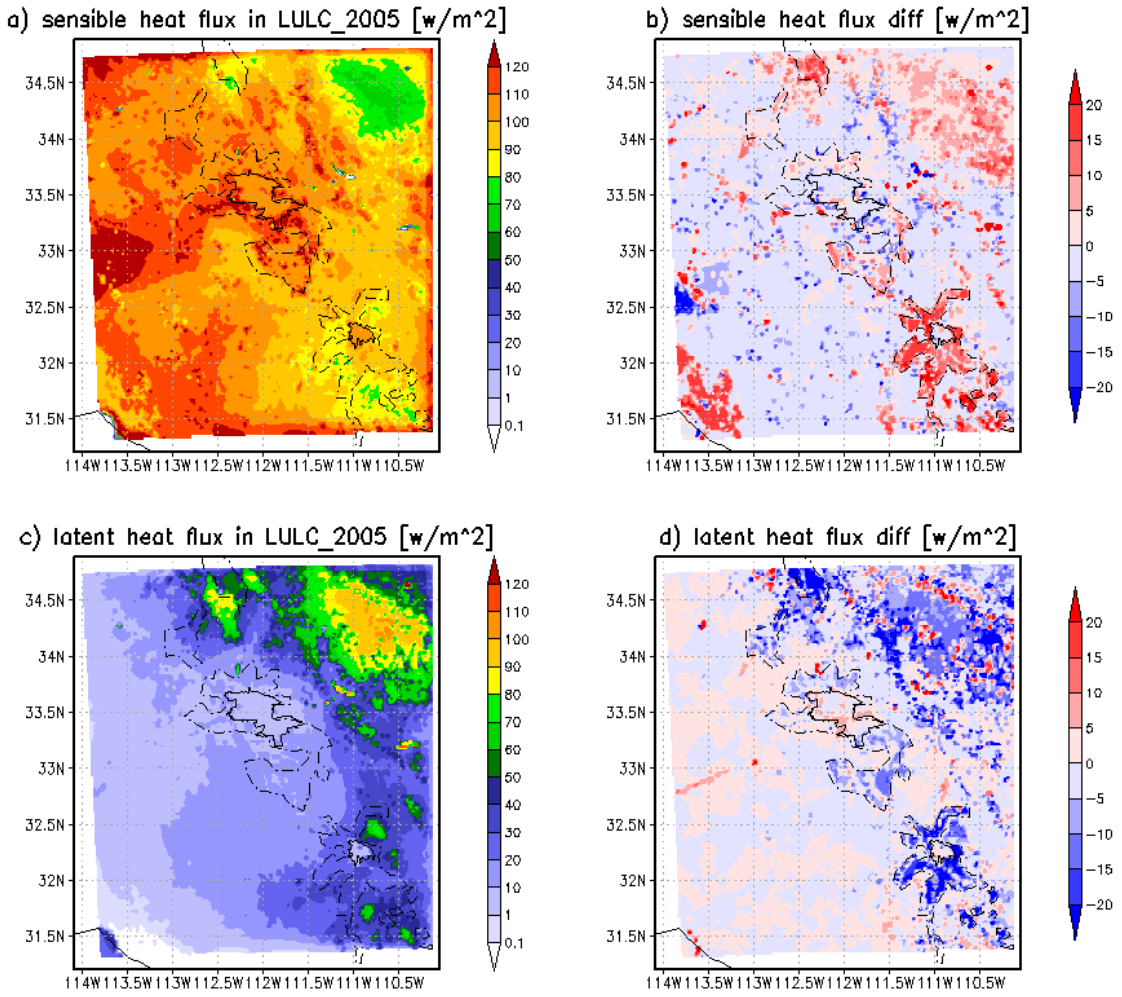

Figure s1: a) Average sensible heat flux in July and August from 1991 to 2000 in LULC_2005. b) Average sensible heat flux difference between LULC_2050 and LULC_2005. c) Similar to a) but for latent heat flux. d) Similar to b) but for latent heat flux difference.

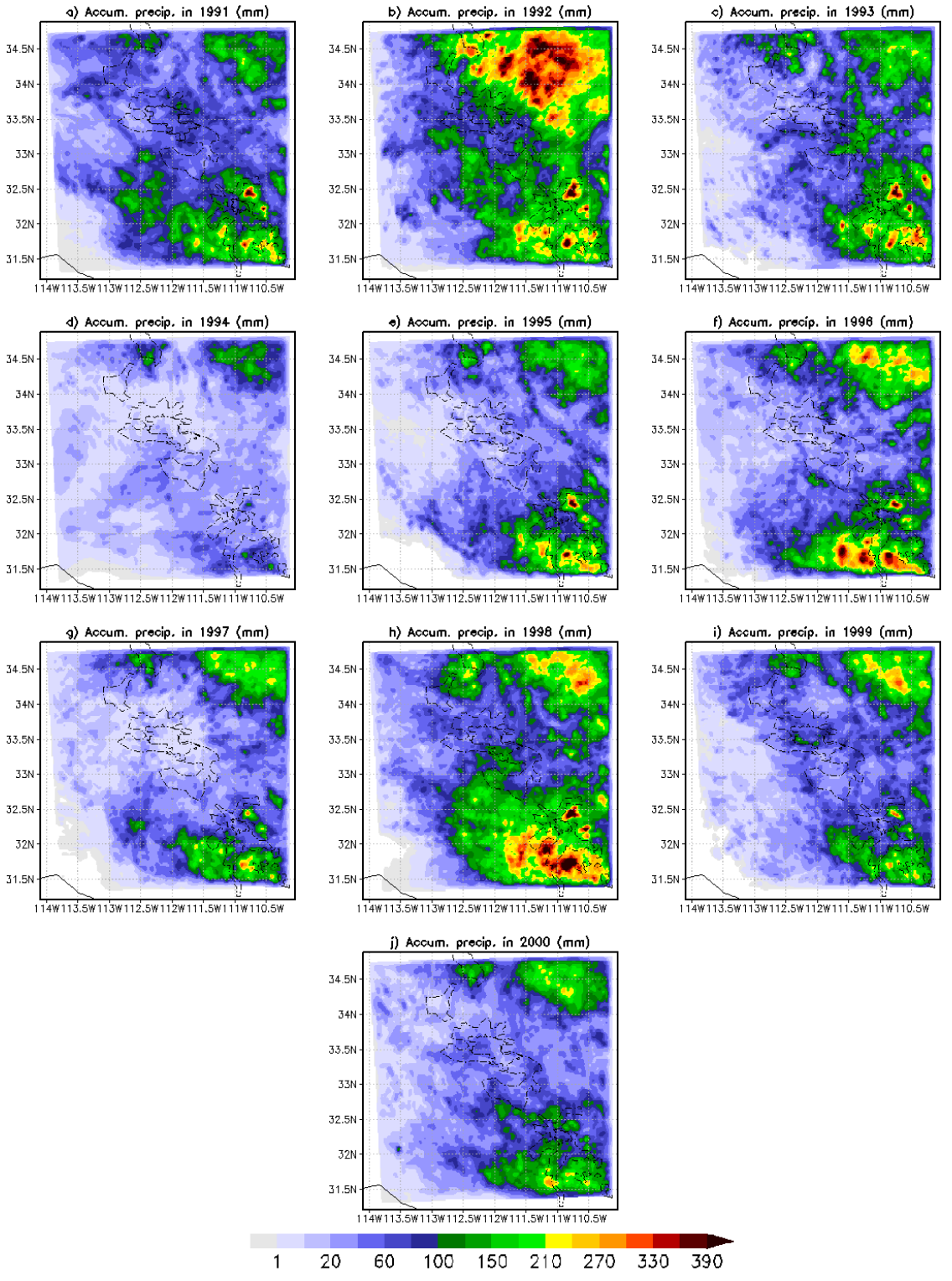

Figure s2: Simulated July and August precipitation pattern from 1991 to 2000 with landscape representation LULC_2005.

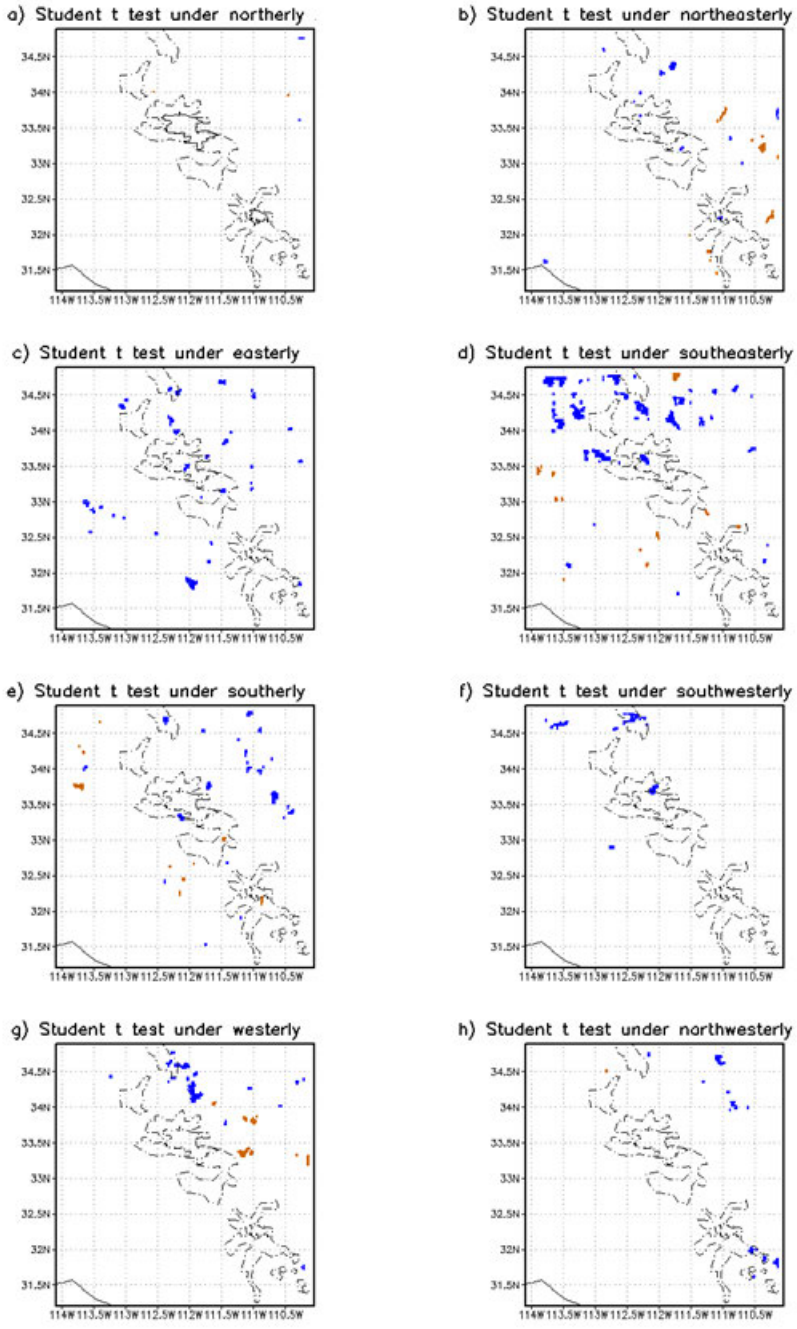

Figure s3: Difference of mean test for precipitation under each flow regime, no significant pattern observed.